Gravitational Deformation Effects: The Yebes 40-m Telescope Case

Axel Nothnagel[1], Anne Springer[1], Erik Heinz[1], Thomas Artz[1], Pablo de Vicente[2]

Abstract The determination of gravitationally induced deformation effects of the parabolic mirror of a radio telescope on the VLBI group delays is closely related to the concept of illumination functions. In our study, these serve as a weighting function of the individual rays in the coherent integration of phase and amplitude at the focal plane of the feed horn. An introduction to illumination functions precedes the manuscript for a better understanding of the implications.
A ray tracing program has been developed and is further extended at the Institute of Geodesy and Geoinformation of the University of Bonn, Germany. This is used to calculate an effective path length from the individual lengths of the rays for the undeformed and the deformed case considering gravitational deformation effects at different elevation angles. After having looked at the Effelsberg 100-m radio telescope in a previous study, we now investigate possible applications of the deformation model for the Yebes 40-m telescope near Madrid, Spain. A preliminary correction model is developed which can be applied for alignment of the station height results of sessions with and without deliberate sub-reflector shift which were employed for gain optimization.

Keywords Radio telescopes, gravitational deformation, illumination function, YEBES40M

1. Institut für Geodäsie und Geoinformation der Universität Bonn, Germany
2. Yebes Observatory, Instituto Geográfico Nacional, Spain

1 Introduction

In recent years, the effect of gravitational deformation has gathered some attention in a few publications, e.g., [4, 5, 6]. Abbondanza and Sarti (2010) [2] investigated illumination functions as weighting function of the individual rays in the coherent integration of phase and amplitude at the focal plane of the feed horn. This weighting function is an important part of a ray tracing program which has been developed for the 100-m Effelsberg radio telescope [1]. This program is now extended for the 40-m radio telescope of the Yebes Observatory (Instituto Geográfico Nacional, IGN), near Madrid, Spain.

The reason for this endeavor is twofold: first, as for any other radio telescope with a homologous design, the VLBI delay observations gathered with the Yebes 40-m telescope need to be corrected for the deformation effects due to movements of the main reflector. When we talk about movements in this article, we mean the movements which take place when the telescope is tilted with different elevation angles. Second, on November 11, 2011, the operations of the telescope was changed from an automatic, deliberate elevation-dependent readjustment of the sub-reflector for maximizing the gain to a fixed sub-reflector position throughout all geodetic and astrometric VLBI sessions. Necessarily, this leads to a discontinuity in the site position, especially in the vertical component.

The aim of this investigation is to produce a correction model for gravitational deformations, which can be applied to the observations with deliberate shift of the sub-reflector or with the fixed sub-reflector to align the two incompatible time series of the telescope positions. The basis of this model development are the ray tracing program, the illumination function, and the function of the sub-reflector shift. Prior to November 11, 2011, the model function of the latter was

$$\Delta R_d(\varepsilon)[mm] = -1.0 - 24.0 \cdot \sin(\varepsilon). \quad (1)$$

Today, ΔR_d equals zero, as the sub-reflector is fixed.

2 Illumination Function

The illumination function of a radio telescope is the Fourier transform of the antenna beam pattern of a radio telescope. Assuming that the latter is radially symmetric, the illumination function can, to first order, just be expressed as a two-dimensional function depending on the radial distance of the impact point on the reflector from the vertex or optical axis.

The antenna beam pattern is constructively mostly dependent on the feed horn characteristics. For completeness, it should be mentioned that the telescope itself with, for example, the quadrupod, i.e., the struts holding the sub-reflector, affects the beam pattern as well. The feed horn is in general designed so that the efficiency drops as sharp as possible at the edge of the reflector. For this reason, the drop in level of sensitivity is also called edge taper. The edge taper is the best compromise because feed horns cannot be built with a Dirac function at the edge. Other, equally important reasons for the edge taper are the optimal suppression of sidelobes and the avoidance of signal pick-up from beyond the aperture of the telescope.

Figure 1 shows the basic construction elements of a prime focus antenna with the normalized sensitivity (in logarithmic scale) superimposed at the location of the feed horn, while Figure 2 does the same for a secondary focus telescope. In general, only the part between the optical axis and the edge (taper) is of interest and the situation can be depicted in a two-dimensional plot of the normalized sensitivity w.r.t. the opening angle or linear distance from the optical axis in the form of an illumination function (Figure 3).

The selection of the function itself mainly depends on the available measurements of the beam pattern, i.e., the gain w.r.t. the opening angle. Mostly only one value, the edge taper, is known and the selection of the best function is rather subjective. Abbondanza et al. [2] favor exponential or binomial functions, while Artz et al. [1] have shown that cosine-squared functions may

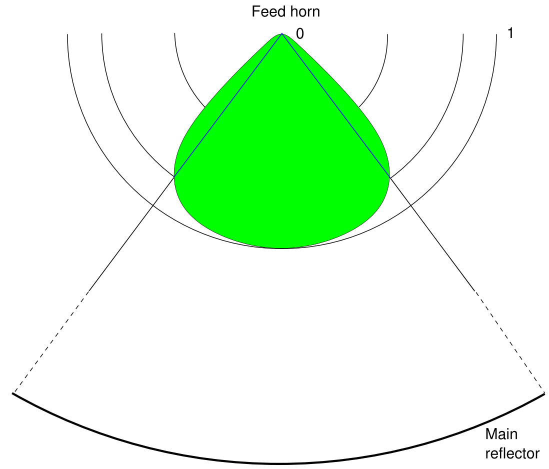

Fig. 1 Prime focus antenna with generic beam pattern. The green/shaded area represents the normalized gain which is "1" towards the vertex of the paraboloid (along the optical axis) and dropping to "0" outside of the reflector area.

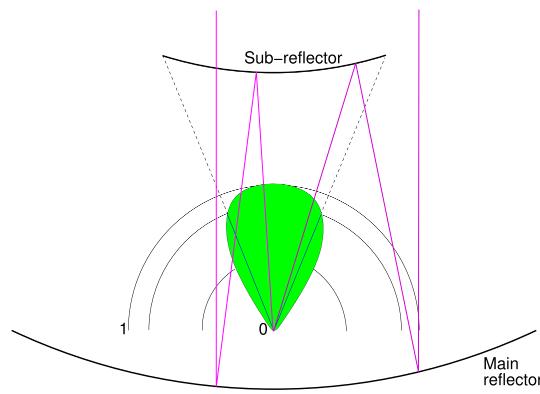

Fig. 2 Secondary focus antenna with generic beam pattern and rays near and away from the optical axis.

be preferable. The most reliable answer to that question can, of course, only be given if the beam pattern has been measured in detail.

3 The Yebes Case

The Yebes 40-m radio telescope of IGN is a secondary focus system with a hyperbolic sub-reflector with a long focal length of the sub-reflector and multiple mirrors in front of the stationary feed horn (Nasmyth system). In an undeformed situation, e.g., at 90° eleva-

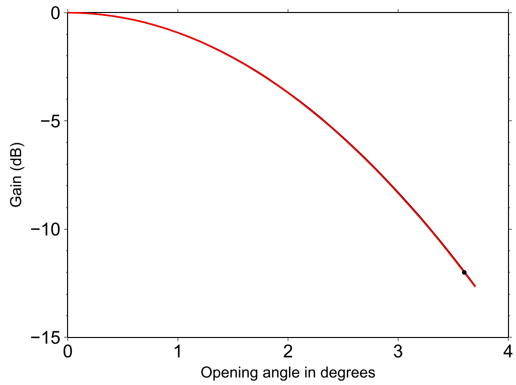

Fig. 3 Gain function of the Yebes 40-m telescope w.r.t. the opening angle of the sub-reflector (γ) for an exponential and a $\cos^2\gamma$ function which cannot be distinguished at this scale.

tion, the telescope geometry is adjusted so that all rays have the same length and are combined in the focal point of the feed horn. To compensate for gravitational deformation effects at other elevation angles, the telescope is built following the homologous deformation concept, i.e., gravitational deformation always leads to a parabolic shape, although with varying focal length, which is the only form parameter of a paraboloid. To compensate for the shift in focal length, an empirical model for movements of the sub-reflector depending on the elevation was determined for optimal gain of the telescope at any elevation angle (Equation 1).

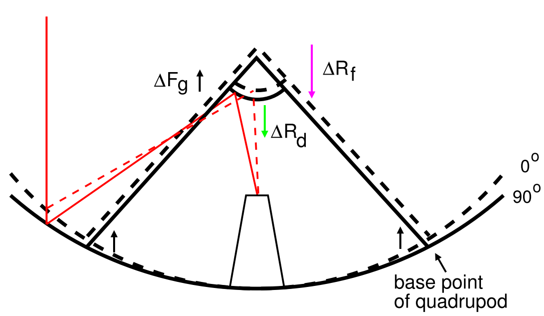

Fig. 4 Form and deformation at 90° and 0° elevation angle with displacement vectors ΔF_g being the focal length change due to gravitation, ΔR_f being the unintended shift of the sub-reflector as a consequence of focal length change through the shift of the base points of the quadrupod and ΔR_d being the deliberate shift coming from empirical gain optimization.

Since no survey of any kind has been carried out at the telescope, only this model for the adjustment of the position of the sub-reflector is known at this point. However, this model does not only comprise the homologous deformation of the paraboloid and the resulting change in focal length. It also includes the unintended gravitational shift of the sub-reflector, which is caused by displacements of the base points of the quadrupod and of the sub-reflector itself through bending of the struts of the quadrupod. So, the deliberate movements of the sub-reflector according to Equation 1 (ΔR_d) compensate for an aggregate of effects which have different impacts on the path lengths of the incoming electro-magnetic rays:

$$\Delta R_d(\varepsilon)[mm] = -(\Delta F_g(\varepsilon) - \Delta R_f(\varepsilon) - \Delta R_g(\varepsilon)), \quad (2)$$

with ΔF_g being the focal length change due to gravitation, ΔR_f being the unintended shift of the sub-reflector as a consequence of focal length change through the shift of the base points of the quadrupod, and ΔR_b being the unintended shift of the sub-reflector due to the remaining gravitational forces.

To deconvolve the three effects, we have to do some reverse engineering. The only solid information which we have right now is how the base points of the quadrupod move as a consequence of the change in focal length. In an iterative process, this shift is computed with the dimensions of the paraboloid and Equation 1, because the same shift applies to the sub-reflector (short black arrows in Figure 4). If we assume that the struts were constructed very rigidly, the remaining gravitational forces on the sub-reflector can be guessed as being negligible.

Computing $\Delta F_g(\varepsilon)$ and $\Delta R_f(\varepsilon)$ from Equation 1 and the dimensions of the telescope, inserting these in the ray tracing program, and applying the illumination function

$$I = -3043.638 + 3043.638 \cdot \cos^2\gamma, \quad (3)$$

with γ being the opening angle w.r.t. the optical axis, permits to compute delay corrections for discrete elevation angles at 10° intervals. A fit to these discrete values yields the continuous correction function

$$\Delta\tau(\varepsilon)[s] = -\frac{1}{c}(51.63 \cdot \sin(\varepsilon) - 0.007 \cdot \cos(\varepsilon) - 51.63 \cdot \sin^2(\varepsilon) - 50.27 \cdot \cos^2(\varepsilon)). \quad (4)$$

This function has its minimum at 90° elevation (0 mm) and a maximum at 0° elevation with

−50.3 mm. It is surprising that a cosine-squared component has such a serious impact on the fit. An explanation is not possible at this time. We can only speculate that it has to do with the fact that the effect amplifies through the aperture of the telescope which goes by the square.

4 Impact on the VLBI Solutions

Finally, the model according to Equation 5 was applied in a standard VLBI solution to all sessions after November 11, 2011, with the Yebes 40 m coordinates being treated as arc parameters. Then, differences to the results of a reference solution without these corrections were computed and depicted in Figure 5. At first

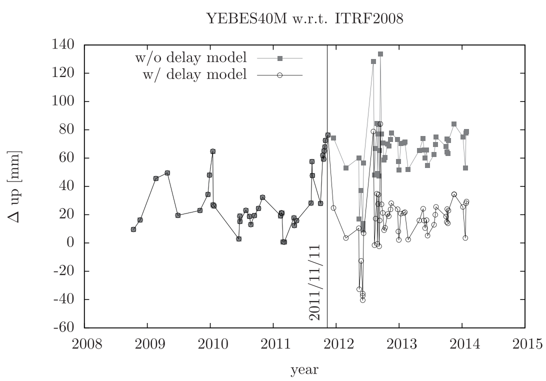

Fig. 5 Relative local height components of the Yebes 40-m telescope with and without delay corrections for deliberate sub-reflector movements.

glance, the obvious jump of approximately 50 mm in the vertical position in the original series after November 11, 2011, definitely disappeared applying the corrections. Most of the corrected data points pretty well match the height level of the 2008 and 2010 results. However, just prior to November 11, 2011, there seem to be a few sessions which might belong to the group of sessions with fixed sub-reflector as well. Likewise, there are sessions in early and late 2009 or in the middle of 2012 which show extra-ordinary height results and need to be checked. This requires some more tedious investigations.

5 Conclusions

The change in operational procedures at the Yebes 40-m telescope on November 11, 2011, with respect to deliberate movements of the sub-reflector have led to a severe discontinuity in the time series of the height results. The correction model developed in this study seems to compensate correctly for the effect which is caused by gravitational deformation of the paraboloid and the counter-acting deliberate shift of the sub-reflector, but the remaining outliers still need to be investigated for a final confirmation.

In view of the computation of any new International Terrestrial Reference Frame, like ITRF2014, further considerations are necessary. For the final coordinates, the VLBI data needs to be re-analyzed with applying the $\Delta R_f(\varepsilon)$, $\Delta F_g(\varepsilon)$, and $\Delta R_d(\varepsilon)$ corrections to the observations prior to November 11, 2011, while for the sessions thereafter, only $\Delta R_f(\varepsilon)$ and $\Delta F_g(\varepsilon)$ have to be applied.

Of course, in this study we neglected the presumably small contribution of the remaining shifts of the sub-reflector due to a possible bending of the quadrupod support struts. This needs to be verified by local surveys like the ones performed at Medicina [5] or Effelsberg [3].

References

1. Artz T, Springer A and Nothnagel A (2014). “A complete VLBI delay model for deforming radio telescopes: The Effelsberg case.” *J Geod*, submitted
2. Abbondanza C and Sarti P (2010). “Effects of illumination functions on the computation of gravity-dependent signal path variation models in primary focus and Cassegrainian VLBI telescopes.” *J Geod*, 84 (8), 515–525, DOI: 10.1007/s00190-010-0389-z
3. Holst C, Zeimetz P, Nothnagel A, Schauerte W, Kuhlmann H (2012): Estimation of Focal Length Variations of a 100 m Radio Telescope’s Main Reflector by Laser Scanner Measurements. *J Surv Eng*, 138 (3), 126–135, DOI: 10.1061/(ASCE)SU.1943-5428.0000082
4. Nothnagel A, Eichborn M, Holst C (2013): Improved focal length results of the Effelsberg 100 m radio telescope. In: Proceedings of the 21st Meeting of the European VLBI Group for Geodesy and Astrometry, N. Zubko and M. Poutanen (eds.), Reports of the Finnish Geodetic Institute, 2013:1, Kirkkonummi, ISBN: 978-951-711-296-3, Finland, 55–59

5. Sarti P, Abbondanza C, Vittuari L (2009): Gravity-dependent signal path variation in a large VLBI telescope modelled with a combination of surveying methods. *J Geod*, 83 (11), 1115–1126, DOI: 10.1007/s00190-009-0331-4
6. Sarti P, Abbondanza C, Petrov L, Negusini M (2011): Height bias and scale effect induced by antenna gravitational deformations in geodetic VLBI data analysis. *J Geod* 85(1): 1–8